

**PECULIARITIES OF SPATIAL SPECTRUM OF
SCATTERED ELECTROMAGNETIC WAVES IN
ANISOTROPIC INHOMOGENEOUS MEDIUM**

V. G. Gavrilenko

Department of Radiowave Propagation and Radioastronomy
Nizhny Novgorod State University
23 Gagarin Ave., Nizhny Novgorod 603950, Russia

G. V. Jandieri

Physics Department
Georgian Technical University
77 Kostava Str., 0175 Tbilisi, Georgia

A. Ishimaru

Department of Electrical Engineering
University of Washington
FT-10 Seattle, Washington 98195, USA

V. G. Jandieri

Graduate School of Science and Technology
Department of Electrical and Computer Engineering
Kumamoto University
Kurokami, Kumamoto 860-8555, Japan

Abstract—Features of spatial power spectrum (SPS) of scattered radiation in a randomly inhomogeneous medium with strongly prolated anisotropic inhomogeneities of dielectric permittivity are investigated. In single scattering approximation, it has been shown that a pronounced gap along a direction of prolate inhomogeneities appears in SPS. Features of SPS of multiple scattered waves at oblique illumination of a boundary of randomly-inhomogeneous medium with prolate irregularities have been analytically studied using smooth perturbation method taking into account diffraction effects. Numerical calculations have shown that with an increase of a distance passing by

the wave in random media, SPS has a double-peaked shape and a gap substantially increases. Its maximum is slightly changed and the width is broadening. The results have been obtained analytically for the first time and could find extensive practical application in optics and be useful in development of principles of remote sensing of random media.

1. INTRODUCTION

Features of EM wave propagation in randomly inhomogeneous media have been intensively studied during the last few decades [1,2]. In the most papers devoting to this problem, statistically isotropic large-scale irregularities are considered. However, in many practical cases, electromagnetic radiation is scattered on irregularities, whose cross-section depends on direction of an incident wave.

Let us analyse some features of narrow-angle scattering radiation by prolate irregularities. One such example is the scattering of X-ray emission by molecules of thermotropic liquid crystals. Characteristic length of these molecules is about 20 \AA and the ratio of longitudinal to transverse sizes equals to $4 \div 8$ [3]. Larger structures are formed in lyotropic systems, where the ratio may exceed 15 [3]. Narrow-angle scattering of ultraviolet radiation is peculiar to chloroplasts. Chloroplasts of algae and plants are ellipsoidal in shape with a diameter $1 \div 5 \text{ \mu m}$ and length of $1 \div 10 \text{ \mu m}$ [3]. Very often prolate irregularities are oriented along a certain direction. Orientation of this kind is observed in lyotropic liquid crystals with hexagonal structure [3]. In thermotropic liquid crystals it can be easily produced by an external electric field. Moreover, it is well known that polymer macromolecules are oriented in a flow of liquid with a velocity gradient [4,5].

Obtained results of this paper could also find extensive practical application in propagation of short-wavelength radiowaves in the Earth's ionosphere, where random plasma inhomogeneities are aligned with the geomagnetic field [6]. Similar scattering effect is observed at propagation of a sound in the ocean, where randomly internal waves exist [7].

2D non-absorptive medium with random irregularities extended along a direction of propagation of an initial wave has been studied in [8]. In this paper, Fokker-Planck equation for the probability density of coordinates and angles of ray-propagation, was derived. The authors have numerically solved the equation and shown that the angular distribution function has a double-peaked shape with a dip along the prolate irregularities.

The features of the angular power spectrum for anisotropic absorptive turbulent magnetized plasma were investigated on the basis of the dispersion equation [9]. Evolution of the angular distribution of ray intensity at light propagation in random medium with prolate irregularities has been investigated in [10,11]. From the results it follows that a local minimum in the angular distribution of ray intensity has been revealed in a direction of the greatest correlation radius of irregularities. Numerical simulation has been carried out by Monte-Carlo method. Many interesting problems in wave propagation have been considered in electrically gyrotropic medium [12–14] and in layered periodic media [15] using dispersion relations.

Within the scope of this paper we investigate the evolution of the angular power spectrum of single-scattered radiation in statistically anisotropic medium. It was shown that strongly pronounced dip exists in angular spectrum along a direction of prolate inhomogeneities caused due to permittivity fluctuations. The same peculiarities have been analytically revealed in SPS of multiple scattered radiation at oblique illumination of medium by mono-directed incident radiation using smooth perturbation method. It has been shown that SPS has a double-peaked shape, location of its maximum slightly varies and the width is substantially broadening in proportion to a distance passing by EM waves in randomly-inhomogeneous medium.

2. SINGLE SCATTERING APPROXIMATION

2.1. Formulation of the Problem

Let a wave field $U(\mathbf{r}, t)$, scalar and monochromatic $U(\mathbf{r}, t) = U(\mathbf{r}) \exp(-i\omega t)$, is incident on a anisotropic turbulent medium. Permittivity $\varepsilon(\mathbf{r})$ is a random function of spatial coordinates $\varepsilon(\mathbf{r}) = \varepsilon_0 + \varepsilon_1(\mathbf{r})$, where ε_0 is the mean value of ε , ε_1 is permittivity fluctuations and the following conditions are fulfilled: $\varepsilon_0 = 1$, $|\varepsilon_1| \ll 1$. Wave propagation in a randomly-inhomogeneous medium satisfies the well-known Helmholtz equation:

$$\Delta U(\mathbf{r}) + k_0^2 [1 + \varepsilon_1(\mathbf{r})] U(\mathbf{r}) = 0, \quad (1)$$

which for small permittivity fluctuations ($\varepsilon_1 \ll \varepsilon_0$), could be solved using the perturbation method. In the expansion of a wave field into the series, we confine only first term U_1 , i.e., scattered field $U \approx U_1$ is a linear functional of $\varepsilon_1(\mathbf{r})$ ($\langle \varepsilon_1(\mathbf{r}) \rangle = 0$), and consequently, correlation function of a scattered field is linearly expressed through the correlation function of inhomogeneities.

Anisotropic Gaussian correlation function is utilized for description a randomly-inhomogeneous medium:

$$V(\mathbf{r}) = \langle \varepsilon_1^2 \rangle \exp \left[-\frac{1}{2} \left(\frac{x^2}{a^2} + \frac{y^2}{b^2} + \frac{z^2}{c^2} \right) \right],$$

where a, b, c are spatial scales of inhomogeneities. Spatial spectrum of a Gaussian correlation function has the form:

$$W(\mathbf{k}) = (2\pi)^{3/2} \langle \varepsilon_1^2 \rangle a b c \exp \left[-\frac{1}{2} (a^2 k_x^2 + b^2 k_y^2 + c^2 k_z^2) \right],$$

where k_x, k_y, k_z are projections of wavevector on x, y and z axes, respectively. Non-Gaussian correlation function has been used in [16] for describing a backscattering mechanism.

Scattering properties of the medium could be modeled in terms of following phase function [11]:

$$\chi(\mathbf{s}, \mathbf{s}') \propto \exp \left\{ -\alpha_{\perp}^2 [(s_x - s'_x)^2 + (s_y - s'_y)^2] - \alpha_{\parallel}^2 (s_z - s'_z)^2 \right\}, \quad (2)$$

where $\mathbf{s} = (s_x, s_y, s_z)$, $\mathbf{s}' = (s'_x, s'_y, s'_z)$ are unite vectors coincident with the direction of the wave-vector of incident and scattered plane waves, respectively; $\alpha_{\perp} = \pi l_{\perp} / \lambda$, $\alpha_{\parallel} = \pi l_{\parallel} / \lambda$ are non-dimensional parameters, λ is the wavelength; l_{\perp} and l_{\parallel} are transversal and longitudinal scales of permittivity inhomogeneities, respectively. Phase function satisfies the normalizing condition:

$$\int_{4\pi} ds \chi(\mathbf{s}, \mathbf{s}') = 4\pi.$$

In the following section, we shall consider single scattering of a plane waves on: a) stretched inhomogeneities along certain direction; b) on disordered inhomogeneities.

2.2. Scattering of Radiation on Strongly Prolated Irregularities Oriented along a Certain Direction

Let a plane monochromatic wave with some disorders of direction of wave-vector is incident on a plane-parallel layer of a randomly-inhomogeneous medium. We shall assume that the following condition $l_{\perp}, l_{\parallel} \gg \lambda$ is satisfied. Irregularities are strongly elongated towards Z -axis and are symmetrical in XY plane. In this case, intensity of a scattered field $I(s'_x)$ in a plane $s'_y = 0$ is obtained from (2) by

integration with respect to wavevector of an incident wave:

$$I(s'_x) = A^{-1} \int_{-1}^1 ds_x \int_{-1}^1 ds_y \exp \left\{ -\beta^2 [(s_x - s_{x0})^2 + s_y^2] - \alpha_{\perp}^2 [(s'_x - s_x)^2 + s_y^2] - \alpha_{\parallel}^2 \left(\sqrt{1 - s'^2_x} - \sqrt{1 - s_x^2 - s_y^2} \right)^2 \right\}. \quad (3)$$

Parameter β characterizes disorder of an incident radiation; s_{x0} characterizes inclination angle of an incident wave with respect to Z -axis; normalizing multiplier A corresponds to the maximum value of an integral. We introduce nondimensional anisotropic parameter $\chi = \alpha_{\parallel}/\alpha_{\perp} = l_{\parallel}/l_{\perp}$ for investigation of the evolution of SPS of scattered radiation. Dependence of normalized intensity of scattered field versus the direction of scattered wave for different anisotropic parameters $\chi = 50, 100$ at $\beta = 200, s_{x0} = 0.07, \alpha_{\perp} = 5$ is illustrated in Figure 1. The curves are normalized on their maximum value. The intensity gains a double-peaked shape; it has a maximum in the direction of an incident wave and local maximums correspond to mirror reflected waves [11].

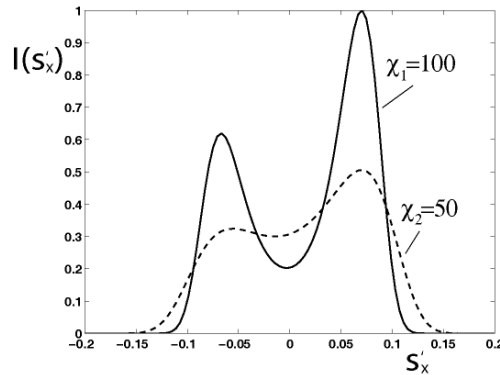


Figure 1. Dependence of normalized intensity of scattered radiation versus the direction of scattered wave at $\alpha_{\perp} = 5, s_{x0} = 0.07, \beta = 200$. Solid curve corresponds to $\chi_1 = 100$, dotted line to $\chi_2 = 50$.

Calculations show, that the gap arises in the direction of prolate inhomogeneities and increases considerably with parameter χ . Figure 2 presents the dependence of normalized intensity of scattered field versus direction of scattered wave for various angles of incidence: $s_{x0} = 0.07$ and $s_{x0} = 0.1$ at the fixed parameters $\chi = 100, \beta = 200$. It could be seen that the amplitude of a reflected wave decreases with

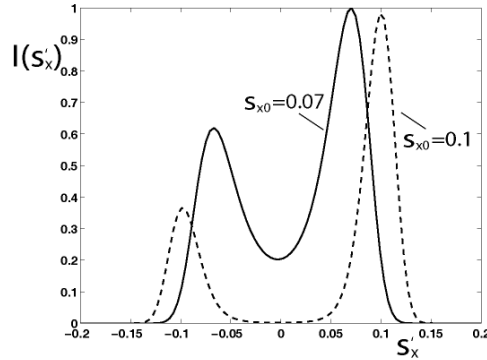


Figure 2. Dependence of normalized intensity of scattered radiation versus the direction of scattered wave at $\alpha_{\perp} = 5$, $\chi = 100$, $\beta = 200$. Solid curve corresponds to $s_{x0} = 0.07$, dotted line to $s_{x0} = 0.1$.

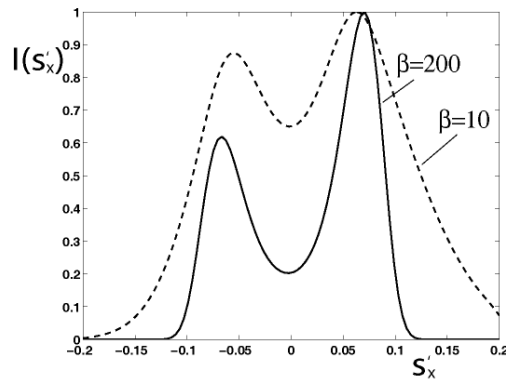


Figure 3. Dependence of normalized intensity of scattered radiation versus the direction of scattered wave at $s_{x0} = 0.07$, $\alpha_{\perp} = 5$, $\chi = 100$. Solid curve corresponds to $\beta_1 = 200$, dotted line $\beta_2 = 10$.

increasing the angle of incidence; maximum of intensity is not changed in magnitude along the direction of an incident wave and is displaced to the right. The gap is broadening but direction of its depth does not vary. The curves of normalized intensity of scattered EM waves for different parameter $\beta = 10; 200$ are presented in Figure 3. It is shown that the dip is getting substantially pronounced in proportion to parameter β and slope of a curve increases. A “double-peaked” shape could be explained by summation of scattered waves, incident on oriented inhomogeneities at different angles. “Double-humping” effect disappears at normal incidence $s_x = 0$ (see Figure 4).

2.3. Incidence of a Plane Wave on Disordered Irregularities

Let a plane wave is incident on disordered inhomogeneities of a randomly-inhomogeneous medium. Intensity of scattered field, in this case, could be obtained from (2) rotating a coordinate system at fixed direction of an incident wave along an unit vector $\mathbf{s}(s_x, s_y, s_z)$,

$$s_z = \sqrt{1 - s_x^2 - s_y^2};$$

$$\begin{aligned} I(s'_x) = G^{-1} \int_0^{2\pi} d\varphi \int_0^\pi d\theta \exp \left\{ -\alpha_x^2 [(s'_x - s_x) \cos \theta \cos \varphi \right. \\ \left. + s'_y \cos \theta \sin \varphi + \left(\sqrt{1 - s'^2_x - s'^2_y} - \sqrt{1 - s_x^2} \right) \sin \theta \right]^2 \\ - \alpha_y^2 [-(s'_x - s_x) \sin \varphi + s'_y \cos \varphi]^2 \\ - \alpha_{\parallel}^2 [-(s'_x - s_x) \sin \theta \cos \varphi - s'_y \sin \theta \sin \varphi \\ \left. + \left(\sqrt{1 - s'^2_x - s'^2_y} - \sqrt{1 - s_x^2} \right) \cos \theta \right]^2 \right\} \exp(-\alpha^2 \theta^2), \quad (4) \end{aligned}$$

where $\alpha_{\perp} = (\alpha_x, \alpha_y)$ is a linear scale of anisotropic irregularities in XOY plane; normalizing multiplier G corresponds to maximum value of an integral; parameter α characterizes disorder of inhomogeneities over the polar angle θ at uniform distribution over the azimuth angle φ . Scattering is observed in plane $s'_y = 0$. Calculations can be carried out also in a curvilinear coordinate system using the relation between polar and bipolar coordinates [17].

We are investigating dependence of the angular spectrum of intensity of scattered radiation in case of chaotically oriented inhomogeneities versus parameter α . Numerical calculations have been carried out at the following fixed parameters $\alpha_x = \alpha_y = \alpha_{\perp} = 5$, $\alpha_{\parallel} = 500$. Curves at $\alpha = 1$ and $\alpha = 10$ are presented in Figure 5. Numerical calculations illustrate that at normal incident ($s_x = 0$) peak of intensity is located in direction of prolate inhomogeneities and has a symmetrical shape; width of an angular spectrum increases in proportion to parameter α . On the other hand, at oblique incidence $s_x = 0.2$ (Figure 6) maximum of the curve is displaced. Comparison of the curves presented in Figures 5 and 6 shows that the width of the angular spectrum at a level 0.5 of its maximum, in case of incident plane waves on chaotically oriented inhomogeneities is much less than in case of incident plane waves along the direction of prolate oriented inhomogeneities. From Figure 6 is evident that the width of the angular spectrum at a level 0.5 of its maximum decreases with increasing

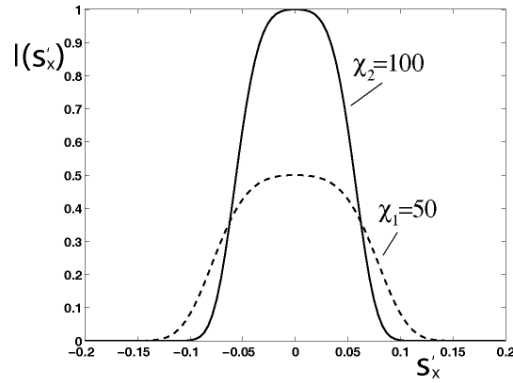


Figure 4. Dependence of normalized intensity of scattered radiation versus the direction of scattered wave at normal incidence of a wave ($s_{x0} = 0$), $\alpha_{\perp} = 5$, $\beta = 200$. Solid curve corresponds to the parameter of anisotropy $\chi_1 = 50$, dotted line $\chi_2 = 100$.

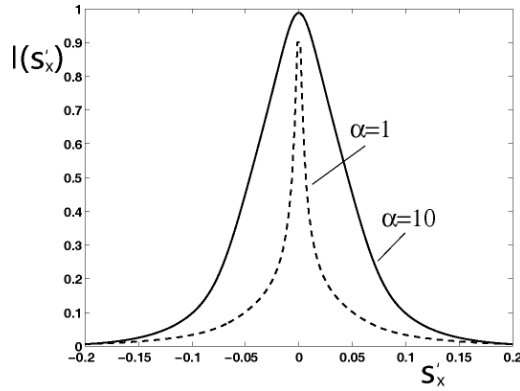


Figure 5. Dependence of normalized intensity of scattered radiation versus the direction of scattered wave at normal incidence ($s_x = 0$), $\alpha_{\perp} = 5$, $\alpha_{\parallel} = 500$. Solid line corresponds to $\alpha = 1$, dotted line to $\alpha = 10$.

a spread of inhomogeneities. We estimate the width of an angular spectrum at a level 0.5 of its maximum ($\Delta\theta_{1/2}$):

- a) for normal incident waves on oriented irregularities: $\Delta\theta_{1/2} \propto \sqrt{\lambda/l_{\parallel}} = \sqrt{\pi/\alpha_{\parallel}}$. Numerical calculations show that at $\alpha = 10$, $\Delta\theta_{1/2} \propto 0.079$, that approximately corresponds to a half-width of a curve $\Delta\theta_{1/2} \propto 0.09$ presented in Figure 5;

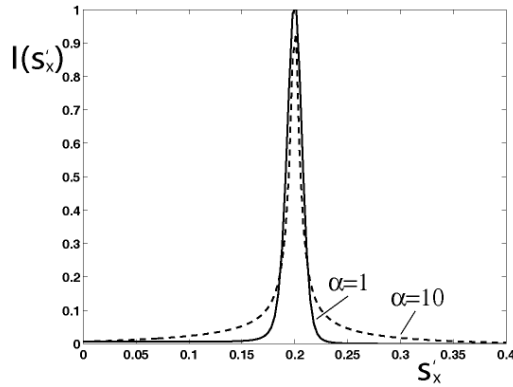


Figure 6. Dependence of normalized intensity of scattered radiation versus the direction of scattered wave at oblique incidence ($s_x = 0.2$), $\alpha_{\perp} = 5$, $\alpha_{\parallel} = 500$. Solid curve corresponds to $\alpha = 1$, dotted line $\alpha = 10$.

- b) for oblique incident waves on oriented irregularities: $\Delta\theta_{1/2} \propto \lambda/l_{\parallel} \cdot s_x$ we obtain $\Delta\theta_{1/2} \propto 0.031$. For a half-width of a curve presented in Figure 6 at $\alpha = 10$, $\Delta\theta_{1/2} \propto 0.017$. Good agreement between estimations and numerical calculations on the basis of formula (4) is obvious.

In this section, we can conclude that SPS in the medium with strongly prolated inhomogeneities along a certain direction substantially depends as on the angle between the wave-vectors of scattered and incident waves as well as on the angle γ between the wave-vector of an incident wave and an axis of prolated irregularities. Phase function at $\gamma = 0$ has a Gaussian form and the maximum coincides with the direction of elongated inhomogeneities (Figure 4). The obtained results are valid for large-scale inhomogeneities $l_{\perp}, l_{\parallel} \gg \lambda$, when observation point is in Fraunhofer zone $l_{\parallel} \cdot \lambda \gg l_{\perp}^2$.

3. MULTIPLE SCATTERING IN RANDOM MEDIUM WITH STRONGLY PROLATE IRREGULARITIES

3.1. Formulation of the Problem

If wavelength λ is small in comparison to the linear scales of permittivity irregularities l_{ε} the scattered waves are concentrated in narrow solid angle θ , i.e., scattered waves are propagating in the same direction as an incident wave. One of the methods describing multiple

scattering in random media is the ray-(optics) approximation, $\sqrt{\lambda L} \ll l_\varepsilon$, but it neglects the diffraction effects. If a distance L passing by the wave in random media is substantially big, diffraction effects become essential. In this case, multiple scattering is effectively described by the smooth perturbation method (narrow-angle scattering) [1, 2]. In this section the features of SPS of multiply scattered EM waves in random medium with strongly elongated irregularities are considered. Dielectric permittivity of medium, as well as in case of single-scattering, we present as $\varepsilon(\mathbf{r}) = 1 + \varepsilon_1(\mathbf{r})|\varepsilon_1| \ll 1$.

Initial is the following scalar wave equation:

$$\Delta E(\mathbf{r}) + k_0^2[1 + \varepsilon(\mathbf{r})]E(\mathbf{r}) = 0. \quad (5)$$

Wave field we introduce as $E(\mathbf{r}) = E_0 \exp\{\Phi(\mathbf{r})\}$, where $\Phi(\mathbf{r})$ is the complex phase, which is presented as a sum $\Phi(\mathbf{r}) = \varphi_0 + \varphi_1 + \varphi_2 + \dots$, $\varphi_0 = ik_0x + ik_\perp y$. At small fluctuations of dielectric permittivity, in the expansion of $\Phi(\mathbf{r})$ we confine only the terms of order ε_1^2 and the wave field could be written as: $E = E_0 \exp(\varphi_1 + \varphi_2 + ik_0x + ik_\perp y)$. We suppose that the following inequalities are satisfied

$$\begin{aligned} \left| \frac{\partial \varphi_1}{\partial x} \right| &\ll k_0 |\varphi_1|, & \left| \frac{\partial^2 \varphi_1}{\partial x^2} \right| &\ll k_0 \left| \frac{\partial \varphi_1}{\partial x} \right|, \\ \left| \frac{\partial \varphi_2}{\partial x} \right| &\ll k_0 |\varphi_2|, & \left| \frac{\partial^2 \varphi_2}{\partial x^2} \right| &\ll k_0 \left| \frac{\partial \varphi_2}{\partial x} \right| \end{aligned} \quad (6)$$

And the system of the differential equations may be written as:

$$\Delta_\perp \varphi_0 + (\nabla \varphi_0)^2 + k_0^2 = 0, \quad (7a)$$

$$\Delta_\perp \varphi_1 + 2\nabla \varphi_0 \nabla \varphi_1 = -k_0^2 \varepsilon_1, \quad (7b)$$

$$\Delta_\perp \varphi_2 + 2\nabla \varphi_0 \nabla \varphi_2 = -(\nabla \varphi_1)^2, \quad (7c)$$

where $\Delta_\perp = \partial^2/\partial y^2 + \partial^2/\partial z^2$. These linear differential equations are solved by Fourier method:

$$\begin{aligned} \varphi_1(x, y, z) &= \int_{-\infty}^{\infty} dk_y \int_{-\infty}^{\infty} dk_z \psi(x, k_y, k_z) \exp[i(k_y y + k_z z)] \\ \varepsilon_1(x, y, z) &= \int_{-\infty}^{\infty} dk_y \int_{-\infty}^{\infty} dk_z f(x, k_y, k_z) \exp[i(k_y y + k_z z)]. \end{aligned} \quad (8)$$

Substituting (8) into (7b) we obtain linear differential equation with respect to ψ :

$$-(k_y^2 + k_z^2 + 2k_\perp k_y) \psi + 2ik_0 \frac{\partial \psi}{\partial x} = -k_0^2 f,$$

whose solution has a following form:

$$\psi(x, k_y, k_z) = \frac{ik_0}{2} \int_{-\infty}^{\infty} d\xi f(\xi, k_y, k_z) \exp\left[-\frac{i}{2k_0}(k^2 + 2k_{\perp}k_y)(x - \xi)\right], \quad (9)$$

$$\mathbf{k} = \{k_y, k_z\}, \quad k^2 = k_y^2 + k_z^2.$$

3.2. Correlation Function and Spatial Power Spectrum

Let us calculate transverse correlation function of a scattered field, $W_{EE^*}(\boldsymbol{\rho}) = \langle E(\mathbf{r})E^*(\mathbf{r} + \boldsymbol{\rho}) \rangle + \langle E(\mathbf{r}) \rangle \langle E^*(\mathbf{r} + \boldsymbol{\rho}) \rangle$ taking into account the fact that the observation points are spaced apart at a very small distance $\boldsymbol{\rho} = \{\rho_y, \rho_z\}$. Second term represents square of the mean field, which we shall not take into account and hence, we have:

$$W_{EE^*}(\boldsymbol{\rho}) = \langle E(\mathbf{r})E^*(\mathbf{r} + \boldsymbol{\rho}) \rangle. \quad (10)$$

Substituting (9) into (8), taking into account that $\langle \varphi_1 \rangle = 0$, exponential terms of the correlation function

$$\begin{aligned} W_{EE^*}(\boldsymbol{\rho}, k_{\perp}) &= E_0^2 \exp(-i\rho_y k_{\perp}) \exp(2 \operatorname{Re} \langle \varphi_2 \rangle) \\ &\cdot \exp\left[\frac{1}{2}(\langle \varphi_1^2(\mathbf{r}) \rangle + \langle \varphi_1^{*2}(\mathbf{r} + \boldsymbol{\rho}) \rangle)\right] \\ &\cdot \exp[\langle \varphi_1(\mathbf{r})\varphi_1^*(\mathbf{r} + \boldsymbol{\rho}) \rangle], \end{aligned} \quad (11)$$

have the following form:

$$\langle \varphi_1^2(\mathbf{r}) \rangle = -\frac{k_0^2}{4} \int_{-\infty}^{\infty} dk_y dk_z dk'_y dk'_z \left(\int_0^x d\xi_1 \int_0^x d\xi_2 X \right), \quad (12)$$

$$\langle \varphi_1^{*2}(\mathbf{r}) \rangle = -\frac{k_0^2}{4} \int_{-\infty}^{\infty} dk_y dk_z dk'_y dk'_z \left(\int_0^x d\xi_1 \int_0^x d\xi_2 Y \right), \quad (13)$$

$$\langle \varphi_1(\mathbf{r})\varphi_1^*(\mathbf{r} + \boldsymbol{\rho}) \rangle = \frac{k_0^2}{4} \int_{-\infty}^{\infty} dk_y dk_z dk'_y dk'_z \left(\int_0^x d\xi_1 \int_0^x d\xi_2 Z \right), \quad (14)$$

where E_0^2 is the intensity of an incident radiation:

$$\begin{aligned} X &= \langle f(\xi_1, \mathbf{k})f(\xi_2, \mathbf{k}') \rangle \exp\left[-\frac{i}{2k}(k^2 + 2k_{\perp}k_y)(x - \xi_1) \right. \\ &\quad \left. -\frac{i}{2k}(k'^2 + 2k_{\perp}k'_y)(x - \xi_2) + ik_y y + ik_z z + ik'_y y + ik'_z z\right], \end{aligned}$$

$$\begin{aligned}
Y &= \langle f^*(\xi_1, \mathbf{k})f^*(\xi_2, \mathbf{k}') \rangle \exp \left[\frac{i}{2k}(k^2 + 2k_{\perp}k_y)(x - \xi_1) \right. \\
&\quad \left. + \frac{i}{2k}(k'^2 + 2k_{\perp}k'_y)(x - \xi_2) - ik_y(y + \rho_y) \right. \\
&\quad \left. - ik_z(z + \rho_z) - ik'_y(y + \rho_y) - ik'_z(z + \rho_z) \right], \\
Z &= \langle f(\xi_1, \mathbf{k})f^*(\xi_2, \mathbf{k}') \rangle \exp \left[-\frac{i}{2k}(k^2 + 2k_{\perp}k_y)(x - \xi_1) \right. \\
&\quad \left. + \frac{i}{2k}(k'^2 + 2k_{\perp}k'_y)(x - \xi_2) + ik_y y + ik_z z \right. \\
&\quad \left. - ik'_y(y + \rho_y) - ik'_z(z + \rho_z) \right].
\end{aligned}$$

Taking into account that $\langle f(\xi_1, \mathbf{k})f^*(\xi_2, \mathbf{k}') \rangle = W_{\varepsilon}(\xi_1 - \xi_2, \mathbf{k})\delta(\mathbf{k} + \mathbf{k}')$, where $W_{\varepsilon}(\xi_1 - \xi_2, k_y, k_z)$ is 2D spatial spectrum of dielectric permittivity fluctuations, δ is Dirac delta function, changing the variables $\xi_1 - \xi_2 = \xi$, $(\xi_1 + \xi_2)/2 = \eta$ and integrating with respect to η , formulae (12)–(14) are finally expressed as:

$$\begin{aligned}
\langle \varphi_1^2 \rangle &= \frac{k_0^2}{4} \int_{-\infty}^{\infty} dk_y dk_z \left(i \frac{k_0}{k^2} \right) V_{\varepsilon} \left(-\frac{k_{\perp}}{k_0} k_y, k_y, k_z \right) \\
&\quad \left[1 - \exp \left(-i \frac{k^2}{k_0} x \right) \right], \tag{15}
\end{aligned}$$

$$\begin{aligned}
\langle \varphi_1^{2*} \rangle &= -\frac{k_0^2}{4} \int_{-\infty}^{\infty} dk_y dk_z \left(i \frac{k_0}{k^2} \right) V_{\varepsilon} \left(-\frac{k_{\perp}}{k_0} k_y, k_y, k_z \right) \\
&\quad \left[1 - \exp \left(i \frac{k^2}{k_0} x \right) \right], \tag{16}
\end{aligned}$$

$$\begin{aligned}
\langle \varphi_1 \varphi_1^* \rangle &= \frac{k_0^2 x}{4} \int_{-\infty}^{\infty} dk_y dk_z V_{\varepsilon} \left[-\frac{1}{2k_0}(k^2 + 2k_{\perp}k_y), k_y, k_z \right] \\
&\quad \exp(-ik_y \rho_y - ik_z \rho_z). \tag{17}
\end{aligned}$$

A term “Re $\langle \varphi_2 \rangle$ ” of (11) is easily calculated by solving a differential equation (7c) utilizing Green function [1, 2]:

$$\text{Re} \langle \varphi_2 \rangle = -\frac{k_0^2 x}{8} \int_{-\infty}^{\infty} dk_y dk_z \left(1 - \frac{k_0}{k^2 x} \sin \frac{k^2 x}{k_0} \right) V_{\varepsilon} \left(-\frac{k_{\perp}}{k_0} k_y, k_y, k_z \right). \tag{18}$$

So, we have calculated all terms for transversal correlation function of a scattered field (11) at arbitrary 3D spatial correlation function of dielectric permittivity fluctuations.

SPS of scattered field in case of incident plane wave $W(k', k_{\perp})$ is easily expressed by Fourier transform of the transversal correlation function [2]:

$$W(k', k_{\perp}) = \int_{-\infty}^{\infty} d\rho_y W_{EE^*}(\rho_y, k_{\perp}) \exp(ik' \rho_y). \quad (19)$$

On the other hand, when the angular spectrum of an incident wave has a finite width, SPS of scattered radiation is given by:

$$I(k') = \int_{-\infty}^{\infty} dk_{\perp} W(k', k_{\perp}) \exp(-k_{\perp}^2 \beta^2), \quad (20)$$

where β characterizes the dispersal of an incident radiation.

3.3. Numerical Results

For numerical simulations, in order to visualize the influence of anisotropy of inhomogeneities on the SPS of scattered waves, we have assumed that anisotropic inhomogeneities are strongly elongated towards Z -axis:

$$V_{\varepsilon} \left(-\frac{k_{\perp}}{k_0} k_y, k_y, k_z \right) = F_{\varepsilon} \left(-\frac{k_{\perp}}{k_0} k_y, k_y \right) \delta(k_z). \quad (21)$$

Substituting (21) into (15)–(18) and integrating over k_z , formula (11) yields:

$$W_{EE^*}(\rho_y, k_{\perp}) = E_0^2 H(k_{\perp}) \exp(-ik_{\perp} \rho_y) \exp \left\{ \frac{k_0^2 x}{4} \int_{-\infty}^{\infty} dk_y F_{\varepsilon} \left[-\frac{1}{2k_0} (k_y^2 + 2k_{\perp} k_y), k_y \right] \exp(-i k_y \rho_y) \right\}, \quad (22)$$

where $H(k_{\perp}) = \exp \left[-\frac{k_0 x}{4} \int_{-\infty}^{\infty} dk_y F_{\varepsilon} \left(-\frac{k_{\perp}}{k_0} k_y, k_y \right) \right]$.

In case of Gaussian correlation function:

$$F_\varepsilon(k_x, k_y) = 2\pi \langle \varepsilon_1^2 \rangle l_{\parallel} l_{\perp} \exp \left[-\frac{1}{2} (l_{\parallel}^2 k_x^2 + l_{\perp}^2 k_y^2) \right], \quad (23)$$

$$H(\mu) = \exp \left[-\sqrt{\frac{\pi}{2}} B (\alpha_1^2 + \mu^2 \alpha_2^2)^{-1/2} \right].$$

transversal correlation function of the scattered field could be rewritten through the non-dimensional parameters:

$$W_{EE^*}(\eta, \mu) = E_0^2 \exp(-i\eta\mu) H(\mu) \exp \left\{ B \int_{-\infty}^{\infty} ds \exp \left[-2s^2 (\alpha_1^2 + \mu^2 \alpha_2^2) - 2\mu\alpha_2^2 s^3 - \frac{1}{2} \alpha_2^2 s^4 \right] \exp(-i\eta s) \right\}. \quad (24)$$

where: $B = \frac{\pi}{2} \vartheta \nu$, $\vartheta = \langle \varepsilon_1^2 \rangle k_0^2 l_{\parallel} l_{\perp}$, $\nu = k_0 x$, $\alpha_1 = \frac{\pi l_{\perp}}{\lambda}$, $\alpha_2 = \frac{\pi l_{\parallel}}{\lambda}$, $s = \frac{k_y}{k_0}$, $\eta = k_0 \rho_y$, $\mu = \frac{k_{\perp}}{k_0}$, $k_0 = \frac{2\pi}{\lambda}$, λ is the wavelength of an incident wave. Dependence of the real part of normalized correlation function $W_{EE^*}(\eta, \mu)$ versus non-dimensional

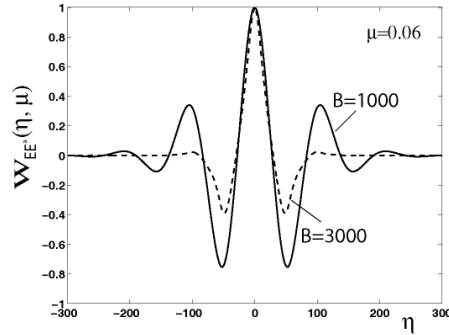


Figure 7. Dependence of normalized correlation function of scattered field $W_{EE^*}(\eta, \mu)$ versus distance between two observation points $\eta = k_0 \rho_y$ at different values of parameter B .

parameter η for $\alpha_1 = 12$, $\alpha_2 = 2000$, $\chi = 166$ are presented in Figures 7 and 8. The curves are normalized on their maximum values and have a symmetrical form. With increasing of distance passing by a wave in a chaotic medium (i.e., with increasing parameter B) $B = 1000$; 3000 correlation function quickly decreases (Figure 7).

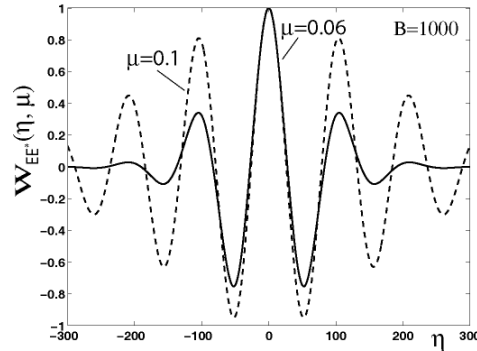


Figure 8. Dependence of normalized correlation function of scattered field $W_{EE^*}(\eta, \mu)$ versus distance between two observation points $\eta = k_0 \rho_y$ at different values of parameter μ .

Location of maximum does not vary and is located at $\eta = 0$. Similar effect is observed at decreasing an incident angle on chaotically oriented inhomogeneities μ (Figure 8).

SPS versus non-dimensional wavy parameter k for fixed anisotropic parameters $\alpha_1 = 12$, $\alpha_2 = 2000$, $\mu = 0.06$ and $B = 1000$; 2000; 3000 is illustrated in Figure 9. Curves are normalized on their values at a point $k = 0.06$. From the numerical calculations it follows that a dip of the curves is getting much more pronounced, location of spectrum maximums slightly varies and the width is substantially broadening with increasing a distance passing by the wave in anisotropic random media. These results are in a good agreement with the results for 3D prolate inhomogeneities calculated by statistical Monte-Carlo method. Numerical analyses show that neglecting diffraction effects, i.e., neglecting the term $k_y^2/2k_0^2$ in the argument of 2D spectrum of dielectric permittivity, “double-humping” effect in SPS disappears.

Finally, we calculated the SPS of scattered radiation, when the incident wave beam has a finite thickness (20). The results are plotted in Figure 10 at $\beta = 10$, $B = 300$; 500; 1000. The curves are normalized, as in previous case, on their values at the point $k = 0.06$. Numerical results demonstrate that the intensity of scattered radiation has a strongly pronounced dip along a direction of prolate inhomogeneities. A dip in SPS is much more pronounced and the maximums are moving apart in proportion to a distance passing by the wave in random media.

The above presented features of multiple scattered radiation of EM wave in random media with prolate inhomogeneities are, for the first time, analytically studied in this paper.

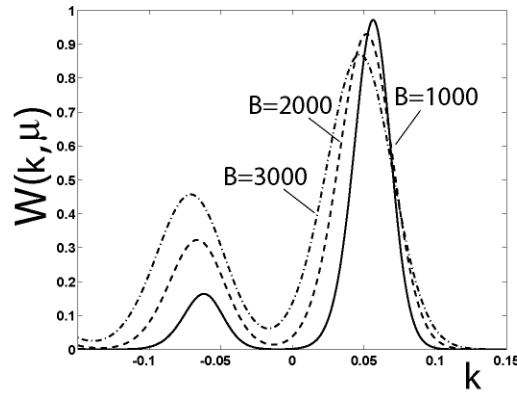


Figure 9. Dependence of SPS (19) versus k for different parameter B at the fixed values $\alpha_1 = 12$, $\alpha_2 = 2000$, $\mu = 0.06$.

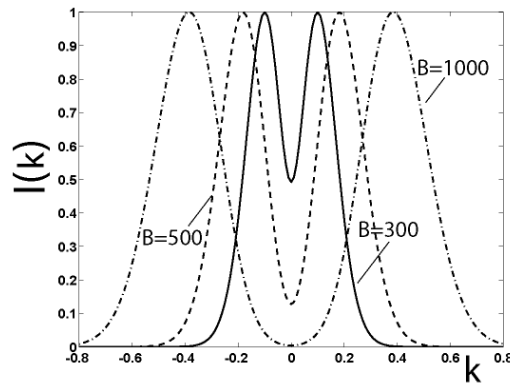


Figure 10. Dependence of SPS (20) versus k for a finite width of an original mode $\beta = 10$, at $\alpha_1 = 12$, $\alpha_2 = 2000$, $\mu = 0.06$.

4. CONCLUSION

Features of SPS of scattered radiation in an inhomogeneous medium with strongly elongated anisotropic inhomogeneities of dielectric permittivity have been studied. Investigation of a single-scattered radiation has shown that strongly pronounced dip appears in SPS of scattered radiation along prolate irregularities when the width of the spectrum of an incident wave substantially exceeds l_{\perp}/l_{\parallel} . Its maximum coincides with the direction of prolate irregularities. Phase function has a maximum towards the direction of incident wave propagation, when axes of elongated random irregularities are chaotically oriented

with respect to the direction of an incident wave. The width decreases with increasing the dispersal of irregularities' orientation and phase function has a sharp peak.

The similar features of SPS could be observed at multiple scattering on prolated inhomogeneities. It has been shown that at the multiple scattering of an oblique incident wave, SPS has a double-peaked shape, its width is substantially broadening and the maxima are slightly changed in proportion to a distance passing by the wave in random media. The behavior of SPS in lossy media [18–20] is under the great interest too.

The obtained results could find extensive practical application in optics and be useful in development of principles of remote sensing of the above-mentioned media.

REFERENCES

1. Ishimaru, A., *Wave Propagation and Scattering in Random Media, Vol. 2, Multiple Scattering, Turbulence, Rough Surfaces and Remote Sensing*, IEEE Press, Piscataway, New Jersey, USA, 1997.
2. Rytov, S. M., Y. A. Kravtsov, and V. I. Tatarskii, *Principles of Statistical Radiophysics, Vol. 4, Waves Propagation Through Random Media*, Berlin, New York, Springer, 1989.
3. Brown, G. H. and J. J. Wolken, *Liquid Crystals and Biological Structures*, New York, 1979.
4. Nakagaki, M. and W. Heller, "Anisotropic light scattering by flexible macromolecules," *J. of Polymer Sci.*, Vol. 38, 117–131, 1959.
5. Eskin, V. E., *Light Scattering by Polymer Solutions and Macromolecule Properties*, Leningrad, Nauka, 1986 (in Russian).
6. Gershman, B. N., L. M. Eruxhimov, and Y. Y. Iashin, *Wavy Phenomena in the Ionosphere and Cosmic Plasma*, Moscow, Nauka, 1984 (in Russian).
7. Flatte, S. M. (ed.), *Sound Transmission Through a Fluctuating Ocean*, Cambridge University Press, London-New York-Melbourne, 1980.
8. Gribova, E. Z. and A. I. Saichev, "On rays diffusion in medium with stretched random inhomogeneities," *Acoustic Journal*, Vol. 39, 1050–1058, 1993 (in Russian).
9. Jandieri, V. G., A. Ishimaru, V. G. Jandieri, A. G. Khantadze, and Z. M. Diasamidze, "Model computations of angular power spectra for anisotropic absorptive turbulent magnetized plasma," *Progress in Electromagnetics Research*, PIER 70, 307–328, 2007.

10. Aistov, A. V. and V. G. Gavrilenko, "The features of light scattering in chaotical medium with prolate irregularities," *Optics and Spectroscopy*, Vol. 83, 427–432, 1997 (in Russian).
11. Gavrilenko, V. G., A. V. Aistov, and G. V. Jandieri, "Some peculiarities of wave multiple scattering in a statistically anisotropic medium," *Waves Random Media*, Vol. 10, 435–445, 2000.
12. Eroglu, A. and J. K. Lee, "Dyadic Green's functions for an electrically gyrotropic medium," *Progress In Electromagnetics Research*, PIER, 58, 223–240, 2006.
13. Eroglu, A. and J. K. Lee, "Wave propagation and dispersion characteristics for a nonreciprocal electrically gyrotropic medium," *Progress in Electromagnetics Research*, PIER, 62, 237–260, 2006.
14. Yesil, A., M. Aydoglu, and A. G. Elias, "Reflection and transmission in the ionosphere considering collisions in a first approximation," *Progress in Electromagnetics Research Letters*, Vol. 1, 93–99, 2008.
15. Sjoberg, D., "Exact and asymptotic dispersion relations for homogenization of stratified media with two phases," *J. Electromagn. Wave and Appl.*, Vol. 20, No. 6, 781–792, 2006.
16. Chen, K. S., A. K. Fung, J. C. Shi, and H. W. Lee, "Interpretation of backscattering mechanism from non-Gaussian correlated randomly rough surfaces," *J. Electromagn. Wave and Appl.*, Vol. 20, No. 1, 105–118, 2006.
17. Costanzo, S. and G. Di Massa, "Direct far-field computation from bipolar near-field samples," *J. Electromagn. Wave and Appl.*, Vol. 20, No. 9, 1137–1148, 2006.
18. Riddolls, R. J., "Near field response in lossy media with exponential conductivity inhomogeneity," *J. Electromagn. Wave and Appl.*, Vol. 20, No. 11, 1551–1558, 2006.
19. Gong, S. H. and J. Y. Huang, "Accurate analytical model of equivalent dielectric constant for rain medium," *J. Electromagn. Wave and Appl.*, Vol. 20, No. 13, 1775–1783, 2006.
20. Li, Y. and P. Yang, "The permittivity based on electromagnetic wave attenuation for rain medium and its application," *J. Electromagn. Wave and Appl.*, Vol. 20, No. 15, 2231–2238, 2006.